

Supporting Information for

## **Biomimic Vein-like Transparent Conducting Electrodes with Low Sheet Resistance and Metal Consumption**

Guobin Jia<sup>1,\*</sup>, Jonathan Plentz<sup>1</sup>, Andrea Dellith<sup>1</sup>, Christa Schmidt<sup>1</sup>, Jan Dellith<sup>1</sup>, Gabriele Schmidl<sup>1</sup>, Gudrun Andrä<sup>1</sup>

<sup>1</sup>Leibniz Institute of Photonic Technology (Leibniz IPHT), Dept. Functional Interfaces, Albert-Einstein-Str. 9, 07745 Jena, Germany

\*Corresponding author. E-mail: [guobin.jia@leibniz-ipht.de](mailto:guobin.jia@leibniz-ipht.de) (Guobin Jia)

### **S1 Error Tolerance of the Leaf Veins**

The leaf vein networks have been ideally optimized for the bi-directional transport function, ensuring the resources to be distributed and collected even if the leaves are damaged due to wormholes as shown in the examples in Fig. S1. However, the leaf cells around the damaged positions are not strongly influenced.



**Fig. S1** Wormholes on *Betula pendula* (a, b) and *Magnolia liliiflora* (c, d) leaves

### **S2 Bi-directional Transport of Water through the Vein Network**

Video S1 demonstrates the water transport from the leaf blade to the petiole.

Video S2 shows the water transport from the petiole to the leaf blade.

### **S3 Determination of the Area of the Veins**

The areas of the veins were determined by drawing the contour of the vein onto a paper with known size (area). Then it was cut out of the paper, and the weight ratio is proportional to the area ratio of the cut piece, so that the area can be determined.

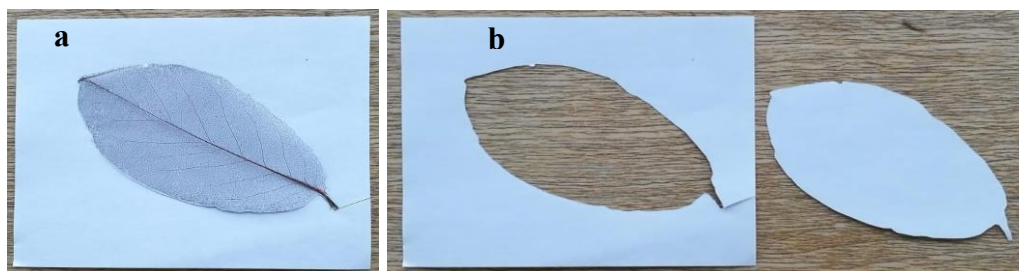


**Fig. S2** a) Draw the contour of the leaf vein on a paper with known size. b) Cut the contour out of the paper and weigh both pieces of the paper. The area of the vein can be determined with the weight ratio.

#### S4 Thickness of the Cu Layer on the Vein

The thickness of the Cu layer is determined by SEM (left) images and the corresponding back scattered electron (BSE) images (right). In the latter case one can distinguish the metal from non-metal as shown in Fig. S3. Due to the irregular shape and rough surface of the veins, it is not possible to measure the thickness accurately. For the 5 and 30 min Cu-plated MLLVs, a thickness of  $\sim 0.5$  and  $5.5 \mu\text{m}$  can be determined from the BSE images, respectively.

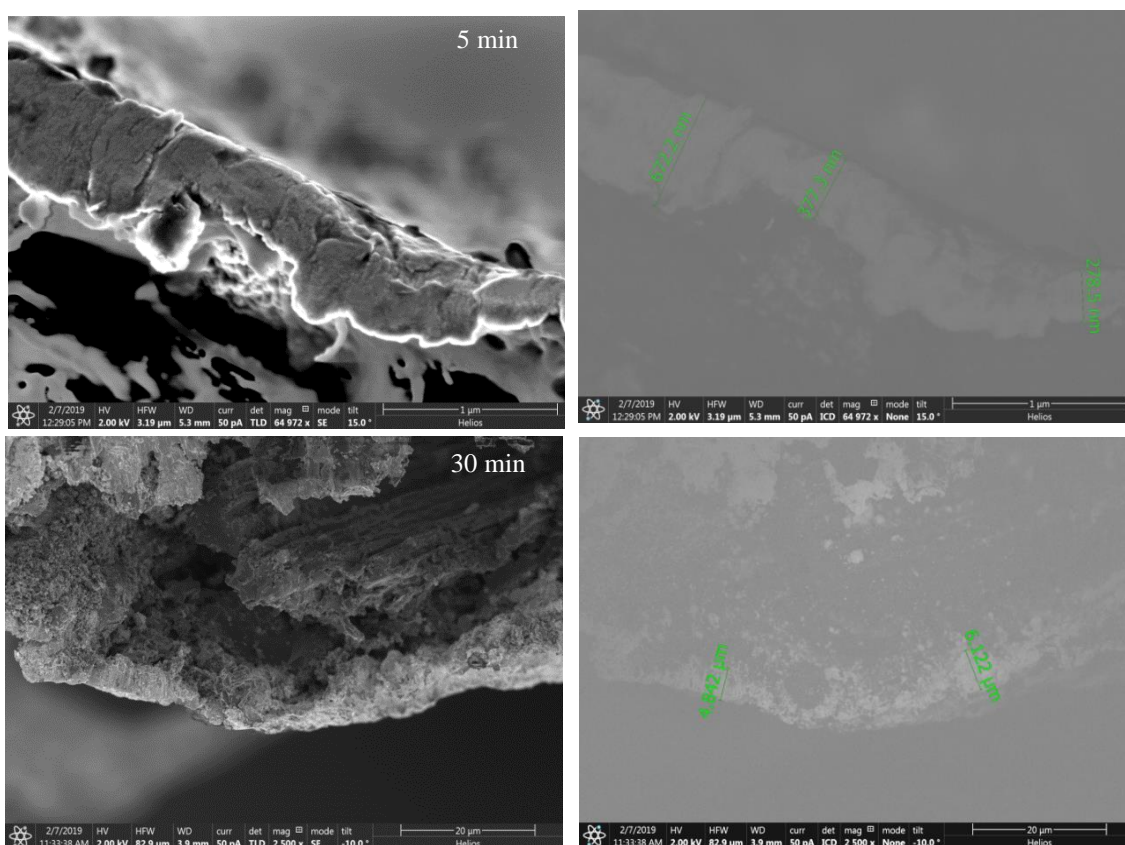


**Fig. S3** Cross-sectional SEM (left) and the corresponding BSE images (right) for 5 min (upper) and 30 min (lower) as-plated MLLV.

#### S5 Annealing of the Veins and the Cu-coated Veins

As-prepared veins as well as 30 min Cu-plated veins (MLLV, *Fagus sylvatica*, and *Populus × canescens*) are placed on quartz glass substrates. They were placed in the tube furnace under

inert N<sub>2</sub>. After 30 min, the furnace temperature was slowly raised ( $\sim 8\text{ }^\circ\text{C min}^{-1}$ ) in several steps:

- Keep at 100 °C for 20 min
- Keep at 150 °C for 30 min
- Keep at 200 °C for 40 min
- Keep at 300 °C for 25 min
- The temperature was raised to 970 °C close to the melting temperature of copper and kept for 120 min.
- The samples were cooled down to room temperature overnight with a continuous flow of N<sub>2</sub>.

By this annealing procedure, the as-prepared vein can be carbonized to a conducting carbon network (Fig. S4a). A resistance of  $\sim 1000\ \Omega$  has been measured on a carbonized MLLV using a multimeter at two points between a distance of  $\sim 2\text{ cm}$ . However, the carbonized network is very brittle and breaks easily during the four-point probe measurement, and so do not allow for systematic measurements. Anyway, we compared similar measurements between two points on the annealed Cu-plated veins with known  $R_{\text{sh}}$ , and estimate that of the carbon network to be at around  $100\ \Omega\ \square^{-1}$ .

Surprisingly, with the Cu-plated veins, mechanically stable networks can be obtained after the annealing. This thermal treatment leads to nearly half of the  $R_{\text{sh}}$  down to an ultralow value of  $68\text{ m}\Omega\ \square^{-1}$  with  $T=85\%$  with the 30 min plated MLLV. After the annealing, a shrinkage of the vein area down to  $\sim 55\%$  can be determined as shown in the examples in Fig. S4b for the 30 min Cu-plated *Populus × canescens* leaf vein on top of a quartz substrate ( $2.5 \times 2.5\text{ cm}^2$ ) before (b) and after (c) the thermal annealing procedure in Fig. S4c.

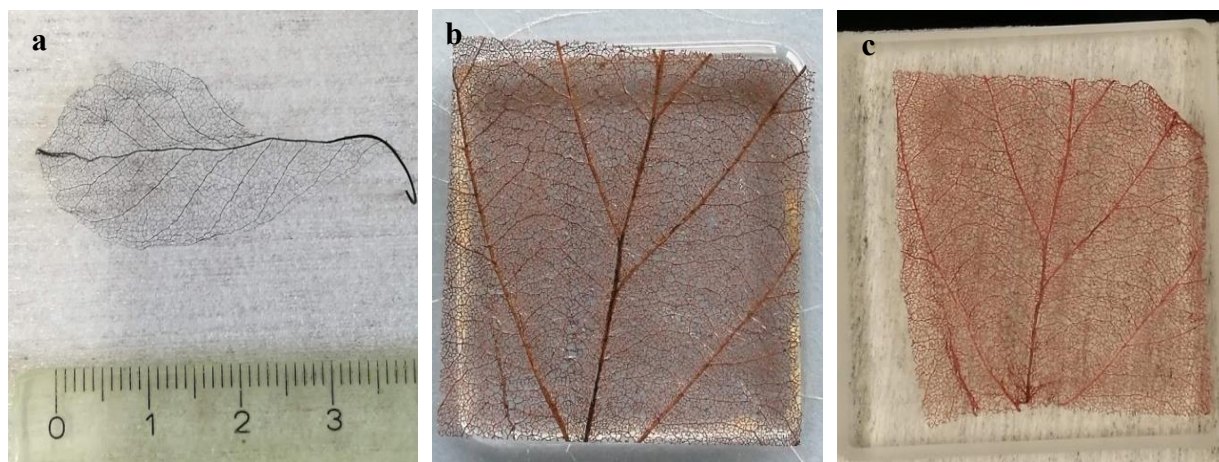


**Fig. S4** Thermal annealing of the vein and Cu-plated veins. **a**) A piece of carbonized (at temperature up to 970 °C) MLLV. **b**) A piece of 30 min Cu-plated *Populus × canescens* leaf vein on top of a quartz substrate ( $2.5 \times 2.5\text{ cm}^2$ ) before (b) and after (c) the thermal annealing

## S6 Results Obtained from *Fagus Sylvatica* Leaf Veins with Higher Vein Density

The *Fagus sylvatica* leaf veins (FSLV) have higher vein densities as shown in comparison with MLLV of Fig. S5a. The 30 min Cu-plated FSLV reaches a  $R_{\text{sh}}$  of  $0.038\ \Omega\ \square^{-1}$  with a  $T=75.2\%$  (value at 550 nm). After the annealing, an exceptionally low  $R_{\text{sh}}$  of  $0.018\ \Omega\ \square^{-1}$  with decreased  $T=61.8\%$  has been reached (see Fig. S5b).



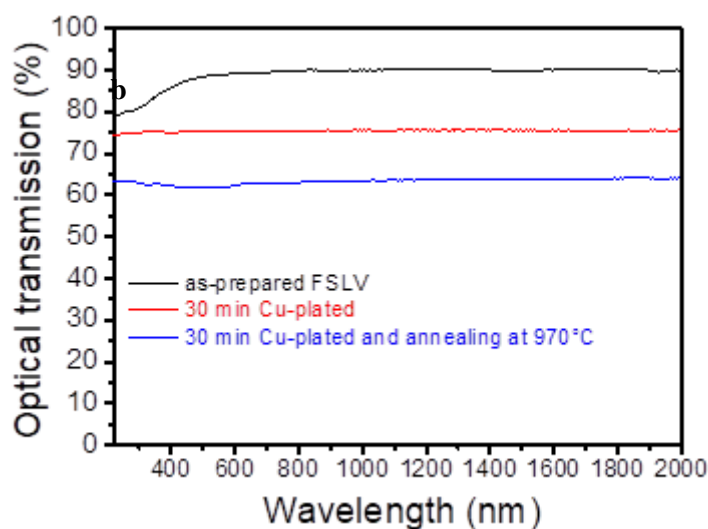
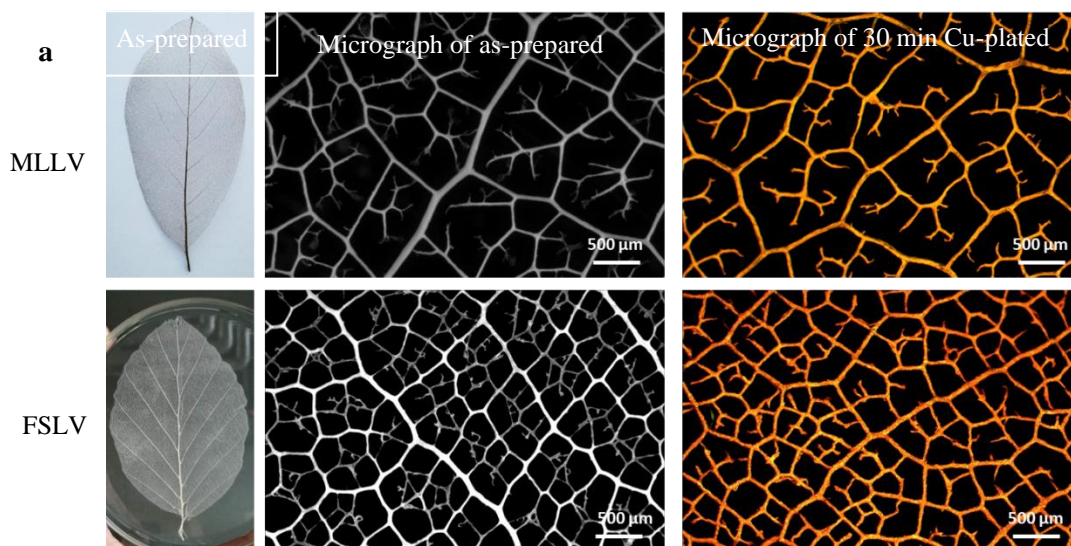


**Fig. S5 a)** Comparison of the MLLV with the dense FSLV in micrographs. **b)** The optical transmissions of as-prepared FSLV (black line), 30 min Cu-plated (red line) and that after the annealing (blue line).

## S7 Surface Morphology

Even after a short plating time of 5 min, a thin layer of copper covering completely the vein network can be seen in the SEM images (Fig. S6).

Cu crystallites are grown on the veins during the ECP forming a compact layer during the ECP even within 5 min. The average crystal sizes of the as-plated samples are in the range of 45-75 nm determined by X-ray diffraction (XRD). A substantial improvement of the crystallinity and growth of larger crystallites up to 140 nm has been determined after the thermal annealing. This can be confirmed by the SEM images in Figs. S7 and S8. The sample annealed at 970 °C show large crystals with clear facets. The improved crystallinity and grown of larger crystals could explain the decrease of the  $R_{sh}$  upon annealing.

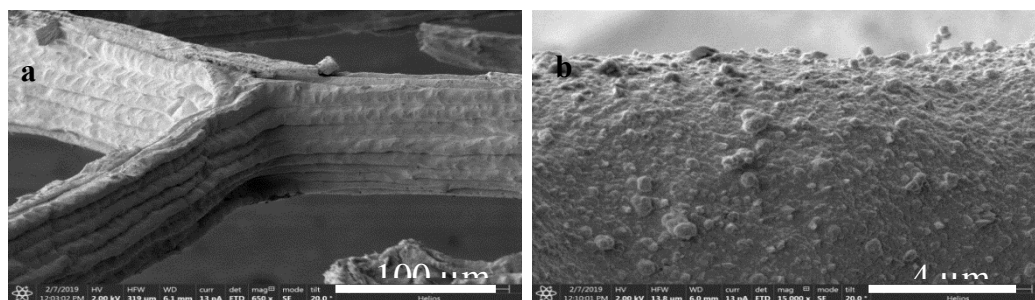


**Fig. S6** a) SEM image of the 5 min as-plated MLLV. b) High resolution SEM image showing a compact layer of Cu crystallites.

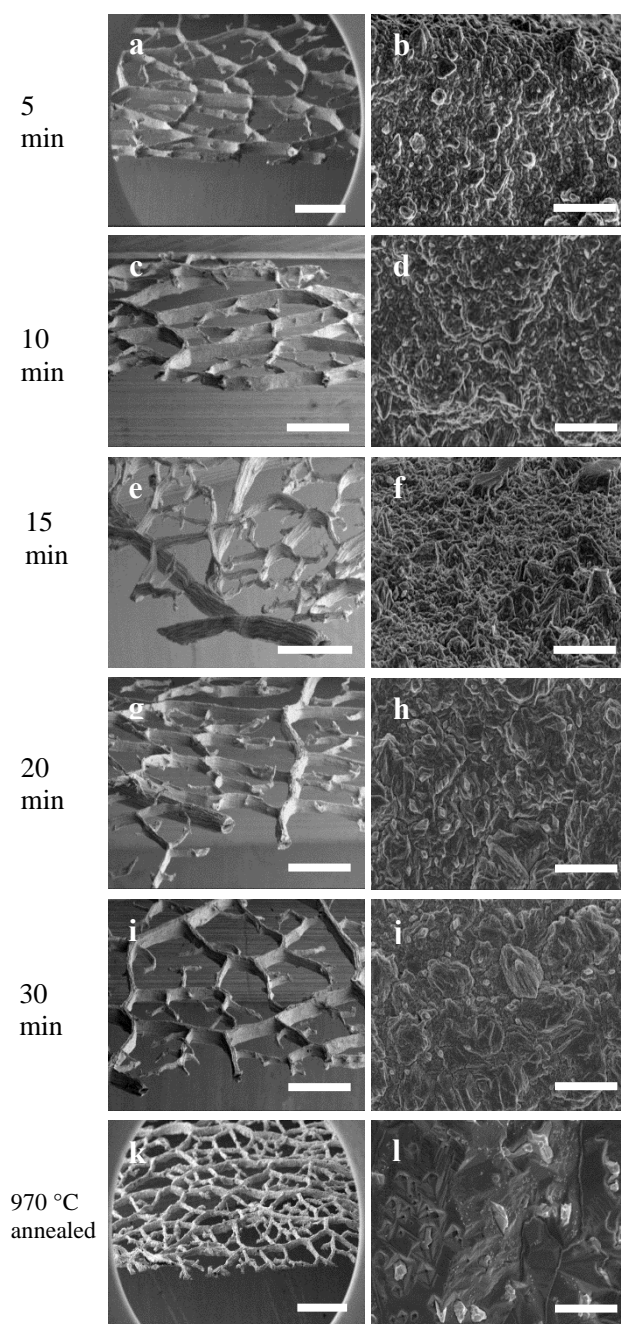


**Fig. S7** SEM overview (left, scale bars: 500 μm) and the corresponding high resolution (right, scale bars: 1 μm) SEM images of the as-plated MLLVs with different plating times and those after the annealing procedure in **k** and **l**



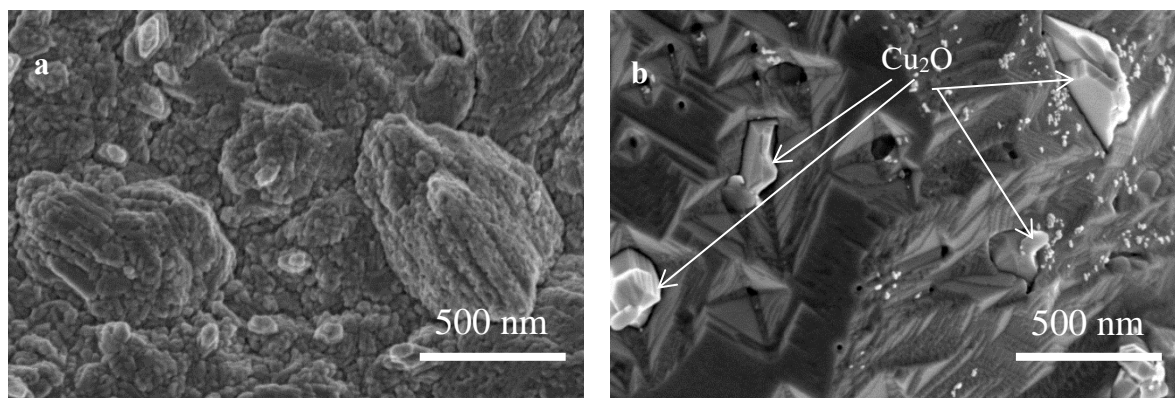


**Fig. S8** Comparison of the morphology of the as-plated vein and that after the annealing procedure. **a)** High resolution SEM image of typical as-plated MLLV (30 min plated). **b)** High resolution SEM image of annealed MLLV showing large crystallites and clear facets on the surface. A small amount of cuprite ( $\text{Cu}_2\text{O}$ ) crystallites are present on the annealed sample.

### S8 Estimation of Current Density

The contact area of the tip is  $0.194 \text{ mm}^2$  (diameter of  $0.88 \text{ mm}$ ) (Fig. S9a), so a  $J$  of  $51.54 \text{ A cm}^{-2}$  passing locally through the two outer tips can be determined. Considering each tip is usually in contact with 6 to 10 of the thin veins as illustrated in Figure S9b, each of them can sustain at least  $10 \text{ mA}$ . From the cross-sectional SEM and the corresponding backscattered electron images (see S6), the thickness of the Cu layer can be estimated to be about  $0.5$  and  $5.5 \text{ }\mu\text{m}$  for the  $5 \text{ min}$  and  $30 \text{ min}$  plated samples, respectively.

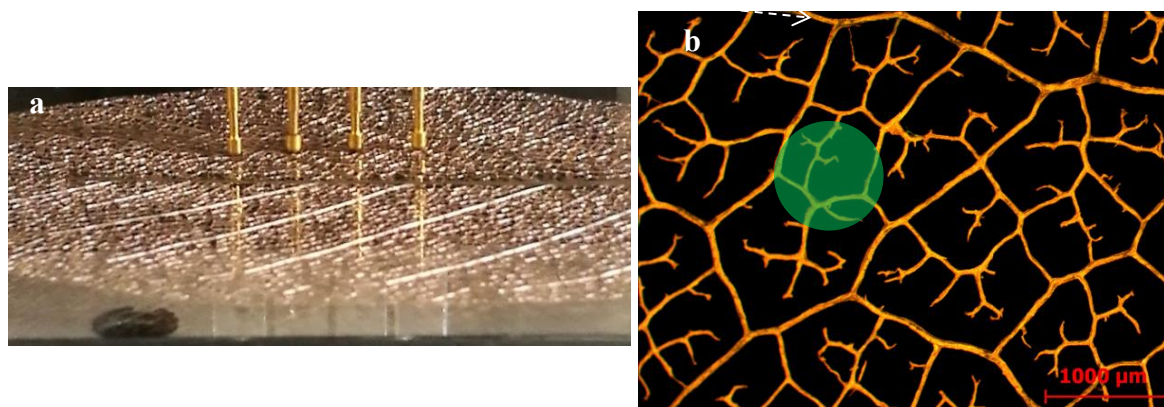


**Fig. S9 a)** A photo showing the as-plated MLLV during the four-probe measurement. **b)** The tips of the four-point probe measurement contacts on the MLLV. Six to ten thin veins could be contacted by the tips with a diameter of  $0.88 \text{ mm}$

Figure S10a, b is SEM image and a sketch of the cross-section of the  $5 \text{ min}$  plated MLLV, respectively. For a conservative estimation of the cross-sectional area of the copper-plated veins, a circle with an equivalent diameter of  $100 \text{ }\mu\text{m}$  of the thin veins is used, considering the rough surface of the veins (Figure S10c), and the cross-sections of the  $0.5 \text{ }\mu\text{m}$  copper layer plated on the  $100 \text{ }\mu\text{m}$  veins can be calculated to be  $\pi(50+0.5)^2 - \pi(50)^2 \approx 158 \text{ }\mu\text{m}^2$ , and that for the  $5.5 \text{ }\mu\text{m}$  copper layer is  $1823 \text{ }\mu\text{m}^2$  (see Figure S10d and S10e). So current densities of  $6329$  ( $5 \text{ min}$  plated) and  $549 \text{ A cm}^{-2}$  ( $30 \text{ min}$  plated) passing through the cross-section of the copper layers can be calculated using the  $10 \text{ mA}$  for each of the thin veins, respectively (noting that a high efficiency solar cell generates a  $J$  of only  $\sim 40 \text{ mA cm}^{-2}$ ).

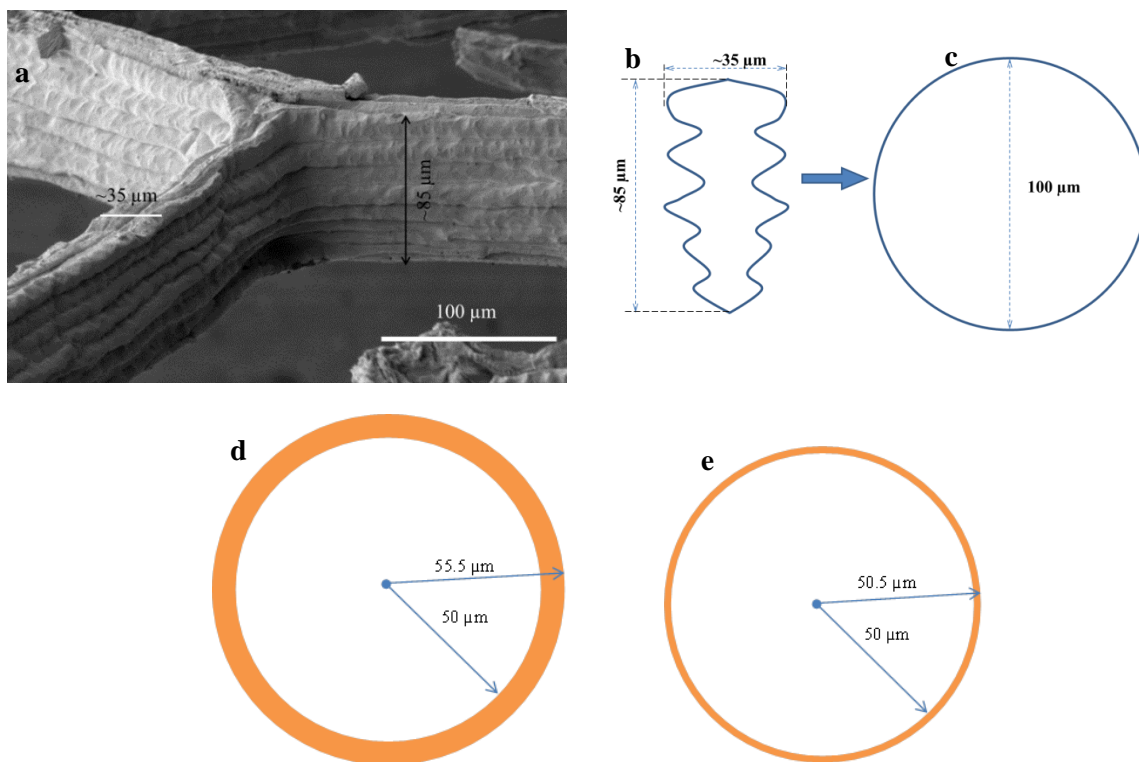


**Fig. S10** a) SEM image of the 5 min plated vein. b) Sketch of the cross section of the vein. c) A circle of 100  $\mu\text{m}$  as the equivalence of the cross section of the vein. d, e Sketches for the calculation of the cross-section of the copper layers with thicknesses of 0.5 (d) and 5.5  $\mu\text{m}$  (e)

### S9 Easy Handling with the Veins and Solderable on a Circuit Board

The Cu-plated veins can be easily handled and even soldered onto a circuit board as shown in the image of Fig. S11a and the micrograph of Fig. S11b. The contact is mechanically stable and gives a very good ohmic conductivity.

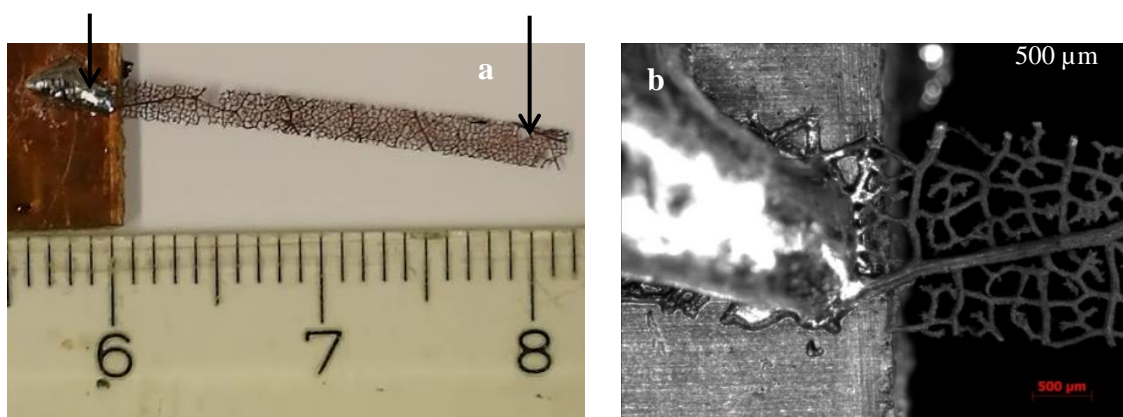


**Fig. S11** a) A stripe of a 30 min Cu-plated MLLV soldered (at  $\sim 350^\circ\text{C}$ ) on a circuit board. A resistance of  $0.8\ \Omega$  is measured between the two arrows. b) The micrographes of the soldered contact.

### S10 Long Term Stability

Oxidation of copper is well-known if it is exposed in air, a thin film of copper oxides will form. To investigate the long-term influence of the oxidation to the sheet resistance, the  $R_{\text{sh}}$  of

some of the Cu-plated MLLVs (5, 10, and 15 min) has been re-measured after one year (379 days), and their sheet resistances keep almost unchanged within the error range. It is noted that these samples were stored individually in closed sample boxes (but not vacuum sealed) in my office.

However, we do have observed increases of sheet resistance for the copper-plated MLLVs stored differently, i. e. sandwiched between two paper sheets. An increase of sheet resistance of 35% (20 min plated) and 31% (30 min plated) have been observed after nearly one year (355 days), respectively, and such results are rather unexpected since these samples have a much thicker copper layers of  $\sim 4$  (20 min plated) and  $5.5 \mu\text{m}$  (30 min plated), a less than 10 nm copper oxides cannot explain the large increase of the  $R_{sh}$  alone. However, in close view to the paper production, it is noticed that a lot of sulfur-containing chemicals are used, and the large increase of the  $R_{sh}$  might well be attributed to the sulfurization of the copper due to sulfur source in the paper.

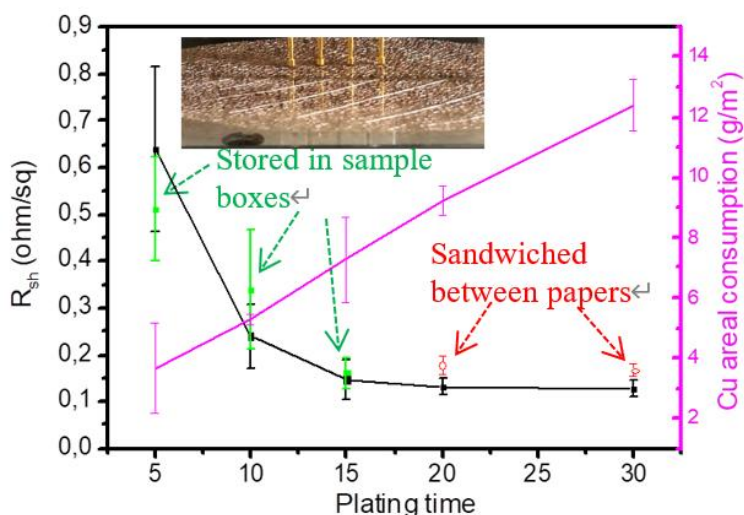


**Fig. S12** The green squares with error bars are copper-plated MLLVs measured after one year (379 days), and the samples were stored individually in sample boxes, and the red circles are those measured after (355 days), which were sandwiched between two paper sheets.

### S11 “Redundancy” of the MLLVs

It is noted that the MLLVs have still many “redundant” free-hanging lower-order thin veins as demonstrated in Fig. S13a. The “redundant” free-hanging lower-order veins have been removed via image processing in Fig. 13b. Obviously, the free-hanging thin veins do not contribute to the measured  $R_{sh}$  since no current can pass through them. They are detrimental to the  $T$  as well as to the Cu consumption for the Cu-plated veins. Nonetheless, the MLLVs demonstrate the excellent ultralow  $R_{sh}$  combined with high broadband  $T$  and low Cu consumption.

Furthermore, the vein networks are only used as framework for the growth of the Cu crystallites on them. If the same amount of copper can be deposited directly onto devices without the framework, for example, by direct 3D printing technology, a greatly reduced thickness of the stems may reach  $R_{sh} \ll 0.1 \Omega \square^{-1}$  with a broadband  $T$  up to 95% .

There is still plenty of room for improving the individual properties for specific applications.



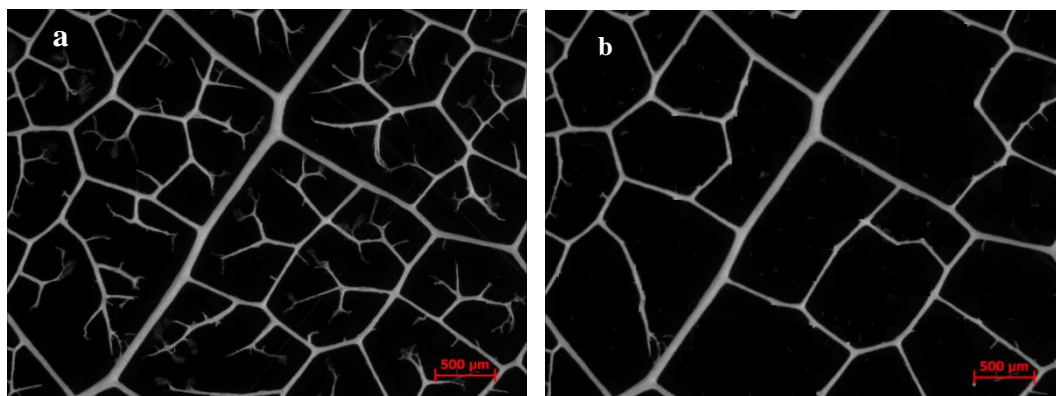


**Fig. S13** **a)** Micrograph of a *Magnolia liliiflora* leaf vein in original state. **b)** Removal of the “redundant” free-hanging lower-order thin veins via image processing.